

# Diagnosing stress state on the welded structure P frame of rotary excavator obtained by thermography, tensometry and fracture mechanics methods

M. Prokolab, Z. Milutinović, N. Marković, D. Jovanović, M. Prvulović, J. Ignjatović, I. Vasović

Institute Goša d.o.o., Milana Rakića 35, 11000 Belgrade, Serbia

E-mail: milan.prokolab@institutgoša.rs

## Keywords

Stress state, welded structures, rotary excavator, P frame, thermography, tensometry, fracture mechanics

## 1. Introduction

Preliminary visual inspection on steel structure P frame of rotary excavator indicated the presence of defects (discontinuities) like cracks or notches. After the visual inspection, standard NDT (EN 571 and EN 1289) and ultrasonic (EN 1712, EN 1713 and EN 1714), had been performed so and dimensional inspection. In assessment of remaining life time, thermography, tensometry and fracture mechanical method are combined.

## 2. Thermography

Stress distribution recording is done by thermography as a screening analysis in order to determine the place of empowerment and setting up the sensors to control. IR camera was used, Terma CAM TM E2, FLIR, with the following characteristics: temperature range from  $-20^{\circ}\text{C}$  to  $250^{\circ}\text{C}$ , thermal sensitivity  $\pm 2^{\circ}\text{C}$ , image frequency 50/60 Hz, spectral range from  $7.5$  to  $13\ \mu\text{m}$ . The research was done by night to minimize the possibility for errors. In addition, the corrections were made for surface emissivity and reflectivity, so and the extinction of air. The thermal stress analysis of steel structures "P" frame, was performed in two conditions: the reference "0" - a condition when the excavator was out of service and working condition when the excavator was in exploitation in all critical digging phases. In the first case we obtained reference values of existing stresses. In the second case of steel structure frame is recorded in the arm moving in the ending positions (either side for  $80^{\circ}$ ) and in the range of optimum digging speed to the maximum. In figure 1. thermograms of the frame parts (measuring point 4) in different stress states are shown. Stress levels are colored as follows: low stress (green), medium stress (blue) and high stress (red). Measuring the temperature difference at selected zones determine points exposed to biggest stresses and strains. These points are measure points, Figure 1.

## 3. Tensometry

The stress distribution obtained by thermography provides an arrangement of measuring gauges (rosettes) in Figure 2, to determine stress and strain values that occur in the steel construction of the P frame when the excavator is operative.

Tensometric tests (measuring gauges and rosettes) are among the most accurate methods of monitoring the process of deformation and stress state in the material. Tensometric tests on steel construction of excavator are made in order to:

- Determine the real deformation and stress state of excavator's steel construction loaded only by its own weight, with different positions of the coal conveyor (back arm).

- Determine the real deformation and stress state of excavator's steel construction loaded only by its own weight and coal digging at different positions of the excavator arms.

The aim of this study is to determine the stresses caused by its own weight (static stress) and exploitation (dynamic stress) in steel construction. Also the aim of this study is evaluation of stress and its intensity in relation with construction's structural integrity.

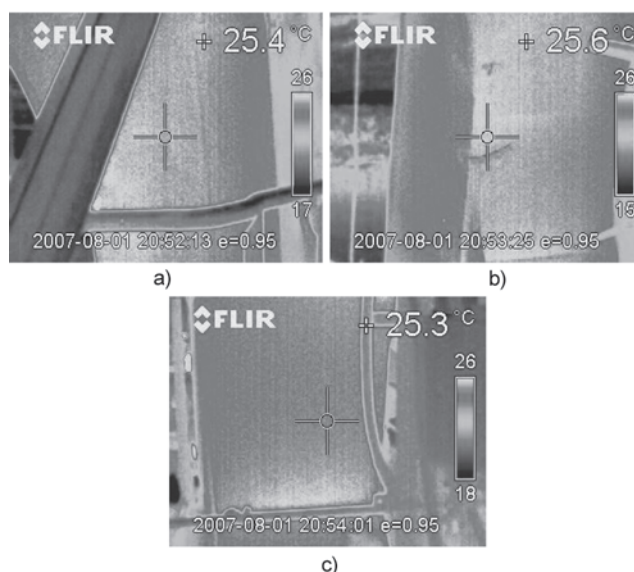


Figure 1. Column, P frame near the top: a) unloaded; b) loaded, ending left position; c) loaded, ending right position

In order to determine the strain and therefore the stress state in excavator's P frame rosettes 10/120 RY 11 (6 rosettes with 3 measuring gauges) and 2 individual measuring gauges 10/120 LY 11, Figure 3.

Measuring amplifier with 8 channel was used (SPIDER-8, HMB) was used for the power supply conditioning measuring points in terms of measuring dynamic (working) load. Measuring amplifier SPIDER-8 was used in an interval of 10 seconds to several minutes to record dynamic load of excavator. Corresponding connector cables, connecting boxes

and personal computer also were used for collecting processing data from individual measuring gauges. At the measuring points where directions of dominant strain were

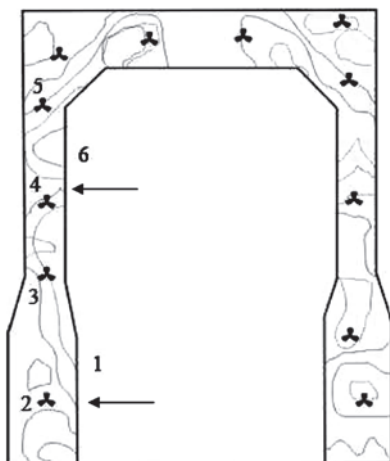


Figure 2. Arrangement of rosettes

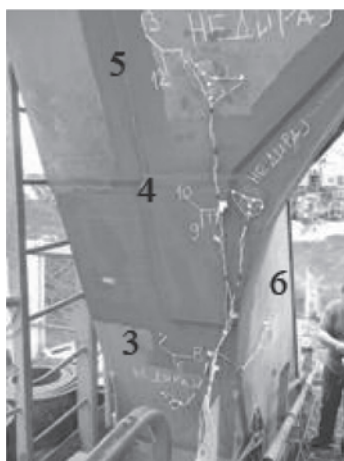


Figure 3. Left column, P frame, measuring points from 3 to 6

known, rectangular rosettes were used. At the measuring points where directions of principal stresses were not known, rosettes were placed (measuring points from 1 to 6).

Based on measured microdeformations by measuring gauge in rosette, principal normal stressess,  $\sigma_1$  i  $\sigma_2$ , principal tangent stress  $\tau_{1,2}$ , and direction of principal stress  $\alpha$  were calculated. The first stage of real strain and stress determination in excavator's P frame was performed in several phases, in relation with back arm position, Table 1.

At few points high stress values are measured.  $\Delta\sigma$  moving up to 178 Mpa at measure point 4., where crack initiated and growth (Table 2). Crack appeared relatively quick, which creates the suspicion that in certain positions of the front and back arm at the stage of digging, dynamic stress is even higher. In the measure points 1 and 2 stress state is the most critical as the result of low cycle fatigue, which results in the appearance of cracks. These cracks are dangerous for the structural integrity of excavator's P frame.

#### 4. Fracture mechanical method

P frame is made from structural steel S355 J2G3 (EN 10025). Examination is performed on sample which is taken from stel construction of P frame, dimensions 300x300x tickness. Tensile

testing on specimens prepared from material taken from P frame is performed at room temperature according to standards EN 10002 i ASTM E8-95. The testing of specimens

Table 1. Phases in relation with back arm position

Phase A	zero state, steel construction of front and back excavator's arm on supporters
Phase B1	construction without supporters, load by its own weight, with lowered front arm, and the back arm up in the horizontal position, 0° relating to the front arm (the coal conveyor)
Phases B2 and B3	construction without supporters, load by its own weight, with lowered front arm, and the back arm up in the horizontal position, 45° and 90° left relating to the front arm
Phases B4 and B5	construction without supporters, load by its own weight, with lowered front arm, and the back arm up in the horizontal position, 45° and 90° right relating to the front arm
Phase B6	construction without supporters, load by its own weight, with lowered front arm, and the back arm up in the maximum position, 0° relating to the front arm
Phases B7 and B8	construction without supporters, load by its own weight, with lowered front arm, and the back arm up in the maximum position, 45° and 90° left relating to the front arm
Phases B9 and B10	construction without supporters, load by its own weight, with lowered front arm, and the back arm up in the maximum position, 45° and 90° right relating to the front arm
Phase B11	determination of deformation and stress state on steel structure P frame of excavator, load by its own weight and coal digging, front arm in different positions

Table 2. Measured microdeformations and calculated stresses-measure point 4

phase	mg9	mg10	mg11	$\sigma_1$	$\sigma_2$	$\tau_{1,2}$	$\alpha,$
	$\mu\text{m}/\text{m}$	$\mu\text{m}/\text{m}$	$\mu\text{m}/\text{m}$	MPa	MPa	MPa	°
A	0	0	1	0	0	0	0
B1	-16	0	4	0	-4	2	15
B2	257	-31	-13	71	6	32	24
B3	357	-42	-24	97	8	44	24
B4	-219	31	23	-3	-59	28	23
B5	-340	58	35	-4	-92	44	24
B6	8	7	17	5	3	1	-25
B7	222	-21	-2	62	8	27	25
B8	370	-38	-17	101	10	45	24
B9	-248	45	33	-1	-67	33	24
B10	-304	57	32	-3	-83	40	24
B11	0	5	9	2	1	1	3

was carried out on the electromechanical testing machine with the displacement and the strain (extension) control at room temperature. The tension speed was 5 mm/min. The extension was registered using a double extensometer. The precision of the extensometer measurement is 0.001 mm.

Analyzing the results of tensile test shows that these results corresponding with the values in standard for steel S355 J2G3 (EN 10025). Stress-strain curve indicate the ductile material with ratio, approximately, 2/3 of homogeneous elongation and 1/3 of non homogeneous elongation. For this purpose following tests are made:

- Charpy impact test;
- Determination of critical intensity stress factor  $K_{Ic}$ ;
- Determination of fatigue crack growth parameters; speed of fatigue crack growth  $da/dN$ , fatigue threshold  $\Delta K_{th}$ , and constants of Paris equation C and m.

Impact test is performed at temperatures (+20°C), 0°C and -20°C on specimen with V-2 notch made from original material taken from P frame, according to standards EN 10045 and ASTM E 23-95.

For full evaluation of material behavior under impact it is necessary to know which part of the energy is spent for crack initiation, and which part of the energy is spent for crack growth. There are several methods for separating the total impact energy,  $A_{uk}$ , on energy for crack initiation,  $A_i$ , and crack growth,  $A_p$ . Most of them are based on the fact that the energy for crack initiation is independent of the radius point, but the radius affects the energy for crack growth. The test temperature is closely related to the plastic properties of the test material. A low temperature induces brittle state and is very characteristic for this type of steel. The total impact energy,  $A_{uk}$  decreases with successive lowering of test temperature from room temperature down to -20°C. However, the effect of rolling texture is almost lost in testing at -20°C.

The total impact energy for specimens of LT direct is 23 J, and for specimens from the TL direct is 22 J. In general, the obtained values of total impact energy and energy components for crack initiation and crack growth energy for specimens taken from the LT and TL direction, show a significant tendency to brittle fracture at low temperature testing, which will be more important in tests of specimens with crack. Specimens for bending test in three points (SEB), defined according to standard BS 7448 Part-1 are proved as very suitable for the practice, so they are the most used. Testing was carried out on electromechanical testing machine at the room temperature. COD test specimen equipped by extensometer is placed on the tool for three-point bending. Bending load is introduced at low speed 0.2 mm / min, so that the one specimen test took about 20min.

The load is introduced with an occasional moment of unloading until the large plastic deformation or rupture of specimen and when the load is out of the extensometer's measurement range.

During this time the A / D converter collected data about the load, displacement (deflection) and the opening of the crack.

The experiments were performed using a test specimen by successive partial unloading, or single specimen compliance method, according to ASTM E1152. Based on results from the tensile testing machine and the COD device, diagram force F - Crack Mouth Opening Displacement  $\delta$  (CMOD) is designed. For SEB specimens elastic component of J-integral, is calculated as:

$$J_{el(i)} = \frac{K_i^2 \cdot (1 - \nu^2)}{E} \quad (1)$$

where:  $K_i$  - intensity stress factor is defined according to standard ASTM E 399,  $\nu$  - Poisson's coefficient and E - modulus of elasticity.

Intensity stress factor  $K_i$  at SEB specimens is calculated as:

$$K_i = \frac{F_i \cdot S}{(B \cdot B_N)^{1/2} \cdot W^{3/2}} \cdot f(a_0/W) \quad (2)$$

Geometric article  $f(a_0/W)$ , at SEB specimens is calculated as:

$$f(a_0/W) = \frac{3(a_0/W)^{1/2} \left[ 1.99 - (a_0/W)(1 - a_0/W) \cdot \left[ 2.15 - 3.93(a_0/W) + 2.7(a_0/W)^2 \right] \right]}{2(1 + 2a_0/W)(1 - a_0/W)^{3/2}} \quad (3)$$

Calculation of fracture mechanics parameters is constructed by J -  $\Delta$  a curve on which is constructed the regression line according to ASTM E1152. Critical J integral is carried out from regression line,  $J_{Ic}$ . If value of  $J_{Ic}$  is known critical intensity stress factor can be calculated or fracture ductility at failure of structure element in domane plane strain deformation,  $K_{Ic}$ , as:

$$K_{Ic} = \sqrt{\frac{J_{Ic} \cdot E}{1 - \nu^2}} \quad (4)$$

Calculated values or fracture ductility at failure of structure element in domane plane strain deformation,  $K_{Ic}$ , are shown in table. 3. Using base equation of fracture mechanics

$$K_{Ic} = \sigma \cdot \sqrt{\pi \cdot a_c} \quad (5)$$

if conventional yield stress  $R_{p0,2} = \sigma$ , with the assumption that value of shape factor is one, approximate values of the critical crack length,  $a_c$ , are calculated, Table 3. After the examination the position of crack caused by specimen bending, crack position is marked. It is done by fatigue or heat treatment on

Table 3. Values of fracture mechanics parameters, measure point 4

Specimen	Critical J- integral, $J_{Ic}$ , kJ/m <sup>2</sup>	Critical intensity stress factor $K_{Ic}$ , MPam <sup>0.5</sup>	The critical crack length, $a_c$ , mm
LT-1	61,4	119,0	36,8
LT-2	67,5	124,8	40,5
LT-3	63,2	120,8	37,9
TL-1	33,8	87,3	19,8
TL-2	29,6	81,7	17,3
TL-3	31,4	84,1	18,4

specimen. It is necessary, because more accurate determination of the total crack length. Specimens have to be broken, that could be measured  $a_0$  initial and final crack length  $a_f$ . Crack front is not parallel to the inlet edge of the specimen Consequently measurements are performed along the 5 to 9 parallel measuring lines, depending on the thickness of the specimen and regularity of the fatigue crack front.

Obtained  $K_{Ic}$  values for specimens taken from the LT direction were at the lower limit of acceptable results for this group of materials, while the specimen from the TL direction considerably lower. These facts classify this steel into the category of materials with low resistance to the presence of crack. ASTM Standard E647 provides measurement of fatigue crack speed  $da/dN$ , which is propagate from the existing crack

and intensity stress factor range,  $\Delta K$ , calculation. This means that the specimen should have a fatigue crack. There are two significant limitations in standard ASTM E647: fatigue crack speed have to be minimum  $10^{-8}$  m/cycle in order to avoid fatigue threshold value,  $\Delta K_{th}$ , and load should be of constant amplitude. The realized frequency was in range from 175 to 195 Hz. It depended from crack direction: through base metal, weld metal or heat affected zone and the value of the load. Medium load and its amplitude are registered to an accuracy  $\pm 3$  Ncm. In order to monitor crack growth using a measuring foil, the device for registering growth of crack FRACTOMAT is used. The system for measuring crack growth, FRACTOMAT and strain gauge are based to register a change of electrical resistance of strain gauges. How fatigue cracks grow below the measurement foils, measuring foil is tearing following the fatigue crack tip and provides a change of electrical resistance of foil, which varies linearly with the change of crack length. The appearance of the prepared specimen for determining the fatigue crack growth is given in Figure 4.

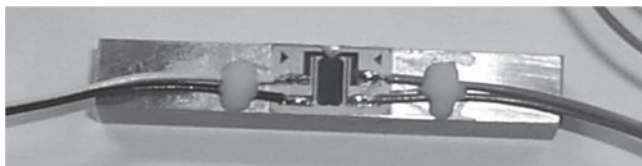


Figure 4. Specimen prepared for testing of speed of fatigue crack growth

Here are calculated values of the parameters of Paris equation, the coefficient C and exponent m, and the fatigue threshold  $\Delta K_{th}$  for all tested specimens. Some results, measuring point 4 is shown in Table 4.

Table 4. Parameters of Paris equation for specimens taken from submitted sample sheet

Specimen	$\Delta K_{th}$ , MPa m <sup>1/2</sup>	Coefficient C	Exp. m	da/dN, m/cycle if $\Delta K=20$ MPa m <sup>1/2</sup>
LT-1	6.1	$4.23 \cdot 10^{-13}$	3.47	$1.38 \cdot 10^{-08}$
LT-2	6.2	$5.32 \cdot 10^{-13}$	3.55	$2.21 \cdot 10^{-08}$
LT-3	6.1	$4.79 \cdot 10^{-13}$	3.41	$1.31 \cdot 10^{-08}$
TL-1	6.1	$2.68 \cdot 10^{-12}$	3.49	$9.31 \cdot 10^{-08}$
TL-2	5.9	$3.11 \cdot 10^{-12}$	3.41	$8.50 \cdot 10^{-08}$
TL-3	5.9	$2.96 \cdot 10^{-12}$	3.46	$9.39 \cdot 10^{-08}$

For different values of stress intensity factor range  $\Delta K$ , which belongs to the validity of Paris equation, we can calculate the fatigue crack growth rate, that the  $\Delta K = 20$  MPam<sup>0.5</sup> ranges from  $1.31 \cdot 10^{-8}$  to  $2.21 \cdot 10^{-8}$  m / cycle for specimens taken from the LT direction and  $8.5 \cdot 10^{-8}$  to  $9.39 \cdot 10^{-8}$  m / cycle for specimens taken from the TL direction. Results shows that the fatigue crack growth rates in TL direction is 5 to 7 times higher than in LT direction, which is a lot of great fatigue crack growth rate and a high tendency to brittle fracture. Fatigue threshold value  $\Delta K_{th}$  ranges from 5.9 MPam<sup>0.5</sup> TL direction to 6.1 MPam<sup>0.5</sup> for the LT direction. These values are within the values that can be found in the literature for this category of materials. When the crack begins to grow, with the same range of stress intensity

factor, it is growing significantly faster in the TL direction than in the LT direction.

The fatigue loads were examined too. The process of fatigue fracture can be classified into three time phases:

- Phase of creation of microcracks and their further growth to the size called engineering crack,  $a_0$ . This may be the minimum crack length, which can be detected, in  $a_{pr}$
  - Stage of stable macrocrack growth to the appearance of instability in the length of  $a_c$ .
  - Unstable phase of growth and final quasistatic fracture.
- Fatigue life prediction for constant amplitude loading and the number of cycles required for crack growth from the initial  $a_0$  to critical  $a_c$  or allowed crack length calculated using the equation 6. Input parameters of test and calculation are as follows:
- $a_0$  is the initial crack detected by nondestructive testing, that is, for example for sheet metal in the zone of the left bearing pole P of steel construction excavator average of 5 mm.
  - Allowable stress range is varied from the most unfavorable case, that is, a stress equal to dynamic strength  $S_f$  of this material, to the real working regime, that is, a stress equal to the maximum measured stress, a certain gage tests on the excavator.
  - Critical length or allowable crack will also vary the size of 5 mm to the size of critical crack length  $a_c$  obtained from fracture mechanics parameters.
  - $C_p$  and  $m_p$  are constants of Paris equation determined by testing the parameters of fatigue crack growth.
  - The coefficient Y is a geometric article who depends on the relationship between the crack length and thickness of sheet metal and is given in the literature for the case of surface cracks and the various relationships  $a / W$ .
  - Annual exploitation period of excavator is about 4500 hours.

$$\Delta N = \frac{1}{C_p [Y \Delta \sigma \sqrt{a}]^{m_p}} \cdot \frac{a_0^{(1-\frac{m_p}{2})} - a_d^{(1-\frac{m_p}{2})}}{\frac{m_p}{2} - 1} \quad (6)$$

Results of the determination of residual life of P frame of excavator, or the number of cycles  $\Delta N$ , until reaching the critical crack length, knowing excavator was loaded by variable load in the work conditions are given in Table 5, for material in which it is assumed that crack propagation in the LT direction in the Table 6 and for the material in which it is assumed that crack propagation in the TL direction. This is important because various characteristics of embedded materials in the presence of crack like defects, or dependence on the direction of crack initiation and propagation.

Based on the measured deformation using a rosette, to calculate the main, auxiliary, and the tangential stress and angle of main stress direction. In this phase of excavator work the largest calculated stress is in measure point 4 (about 190 MPa), in a place where crack is detected, which is why the steel construction of P pole was repair. The maximum operating stress of 190 MPa is the sum of static and dynamic stress measured at the measuring location. How are the conditions of action of dynamic loads determined  $\Delta \sigma$ , we assumed that the maximum applied stresses equal the sum of static stress and half of the dynamic stress.

From the results shown in Tables 5 and 6 can be seen that the remaining life of structural steel column of P frame in exploitation or number of cycles  $\Delta N$  depends on the

placement of notch (if the crack is in the LT or TL direction), the assumed crack length and scope allowable stress.

During one hour of excavator exploitation is noticed average between 150 and 200 significant changes in strain or stress state, which may have some bearing on the structural integrity and residual life of steel construction P frame. These changes in strain and stress state are classified as cycle changes. To reach the critical crack length of 15 mm, requires the exploitation period of 1.55 years. From the study results, presented in Tables 5 and 6, can be seen that the exploitation period of the assumed error are small, as the current phenomenon of initiation and growth of cracks and confirmed.

Table 5. The parameters of residual life of steel structures of P pole-material in the L-T direction, the measure point 4.

Loading case	Geometric Article, Y	Range of allowed stress, $\Delta\sigma$ , MPa	The assumed crack length, a, m	Initial crack length, $a_0$ , m	The critical crack length, $a_c$ , m	Number of cycles, $\Delta N$	Residual expl. Period, the year *
Measure point 4							
I	7,56	245	0,005	0,005	0,038	3556546	3,95
	6,71	245	0,020	0,005	0,038	463724	0,52
	6,11	245	0,030	0,005	0,038	314859	0,35
II	7,56	190	0,005	0,005	0,038	8769861	9,74
	6,71	190	0,020	0,005	0,038	1143467	1,27
	6,11	190	0,030	0,005	0,038	776391	0,86

\* Applies in the case of the initial crack length of 5 mm

Table 6. The parameters of residual life of steel structures of P frame-material in the TL direction, the measure point 4.

Loading case	Geometric Article, Y	Range of allowed stress, $\Delta\sigma$ , MPa	The assumed crack length, a, m	Initial crack length, $a_0$ , m	The critical crack length, $a_c$ , m	Number of cycles, $\Delta N$	Residual expl. Period, the year *
Measure point 4							
I	7,56	245	0,005	0,005	0,015	577184	0,64
	6,71	245	0,010	0,005	0,015	262880	0,29
	6,11	245	0,014	0,005	0,015	203102	0,23
II	7,56	190	0,005	0,005	0,015	1391046	1,55
	6,71	190	0,010	0,005	0,015	633556	0,70
	6,11	190	0,014	0,005	0,015	489487	0,54

\* Applies in the case of the initial crack length of 5 mm

## Conclusion

Application of thermography systems for the analysis of industrial structures has shown that the system is an effective tool for the identification of stress in dynamically loaded structures.

Combining thermography techniques with measurements of stress using strain gauges can lead to great benefit in maintaining these structures.

Microstrains measured by strain gauges and calculate the principal stress, clearly indicate a very unfavorable stress state in the area of measuring points 2, 4 and 6, which results in cracking.

Measuring points 1, 3, and 5 are slightly more favorable stress state, but they represent a potential threat to come to the occurrence of cracks.

Performed based on fracture mechanics testing of the submitted sample plate of the steel structure, can be concluded the following:

- P frame is made of structural steel which does not meet the standard set of values impact properties (total impact energy at -20°C is below 27J)

- The lowest fatigue crack growth,  $da/dN$ , and the highest resistance to crack propagation have specimens taken from the LT direction of the crack in the TL direction, which means that the rolling texture and the direction of crack propagation has a big impact on the integrity and remaining life of steel construction

- In the case of crack initiation, the remaining period of exploitation depends on the level of load in exploitation and crack initiation point.

- The measured values of static and dynamic loads, and stress are enough high and combined with welded joints are real danger for the initiation and further propagation of cracks.

## Acknowledgments

This paper is the result of research within the projects TR 35024 and TR 34028, which is financially supported by Ministry of Science and Technology of Serbia.

## References

- [1]. Kutin, M., Adamović, Ž.: *Tensile features of welded joint testing by thermography*, Defektoskopija, Russian Journal of Nondestructive Testing, No5, 2010.,pp.89-97
- [2]. Kutin M., Ristić S., Puharić M., Burzić Z.: *Tensile features of steel spacemen testing by thermography*, Scientific Technical Review, Vol 60, No. 1, Belgrade, pp.66-70
- [3]. Maksimović S., Kutin M., Maksimović K., Vasović I.: *Crack growth analysis of notched structural components under mixed modes*, 2nd International Congress of Serbian Society of Mechanics, 1-5 June 2009, Palić (Subotica), B-06
- [4]. Ummenhofer T. medgenberg J.: *On the use of infrared thermography for the analysis of fatigue damage processes in welded joints*, doi10.1016/j.ijfatigue.2008.04.005, 2008. International journal of Fatigue, Vol. 31, 0, 2009.,pp.130-137
- [5]. Man-Yong C.I., Jung-Hak P., Ki Soo K., Won-Tae K.: *Application of Thermography to analysis of thermal stress in the NDT for compact tensile specimen*, 12th A-PCNDT 2006-Asia-Pacific Conference on NDT, Auccland, Hew Zealand, 5th -10th Nov. 2006.
- [6]. Byrd L.W., Haney M. A.: *Thermoplastic stress analysis applied to fully reserved bending fatigue*, Experimental Mechanics, 40(1) pp.10-14., Mar. 2000.

